ACS AuthorChoice

Environmental Science & Technology

Article

pubs.acs.org/est

Field Measurements of Black Carbon Yields from Gas Flaring

Bradley M. Conrad and Matthew R. Johnson*

Energy & Emissions Research Laboratory, Department of Mechanical and Aerospace Engineering, Carleton University, 1125 Colonel By Drive, Ottawa, Ontario K1S 5B6, Canada

Supporting Information

ABSTRACT: Black carbon (BC) emissions from gas flaring in the oil and gas industry are postulated to have critical impacts on climate and public health, but actual emission rates remain poorly characterized. This paper presents in situ field measurements of BC emission rates and flare gas volume-specific BC yields for a diverse range of flares. Measurements were performed during a series of field campaigns in Mexico and Ecuador using the sky-LOSA optical measurement technique, in concert with comprehensive Monte Carlo-based uncertainty analyses. Parallel on-site measurements of flare gas flow rate and composition were successfully performed at a subset of locations enabling direct measurements of fuel-specific BC yields from flares under field conditions. Quantified BC emission rates from individual flares spanned more than 4 orders of magnitude (up to 53.7 g/s). In addition, emissions during one notable ~24-h flaring event (during which the plume transmissivity dropped to zero) would have been even larger than this maximum rate, which was measured as this event was ending. This highlights the likely importance of superemitters to global emission inventories. Flare gas volume-specific BC yields were shown to be strongly correlated with flare gas heating value. A newly derived correlation fitting current field data and previous lab data suggests that, in the context of recent studies investigating transport of flare-generated BC in the Arctic and globally, impacts of flaring in the energy industry may in fact be underestimated.

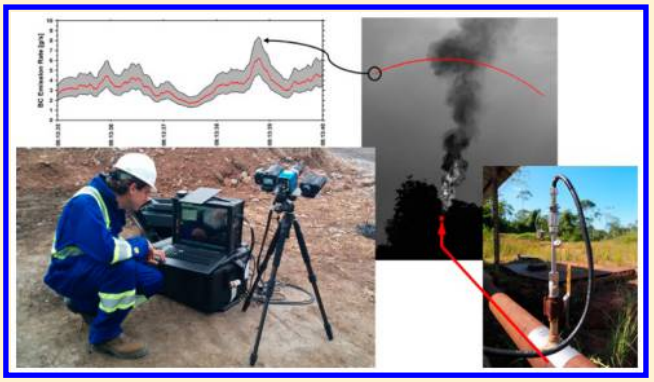

INTRODUCTION

Flaring is a common practice within the oil and gas (OG) industry of combusting extraneous gases in an open diffusion flame, usually at the exit of a vertically raised flare stack or within a refractory-lined pit. Flaring is generally preferred over venting to reduce equivalent greenhouse gas emissions and health and safety risks to the local population. However, the combustion of flared gas produces atmospheric pollutants including soot, which is a form of particulate matter of less than 2.5 μm in diameter ($PM_{2.5}$) consisting of mass-fractal-like aggregates of nanoscale spherules. Black carbon (BC), the carbonaceous component of soot, is an important atmospheric pollutant with critical impacts on local public health and the global environment. Specifically, recent research[1−3] has indicated that BC is a key component contributing to the adverse health effects associated with $PM_{2.5}$, while BC has also been identified as likely the second-most important atmospheric direct radiative forcer (after CO_2).[4,5]

Satellite imagery of flaring activity by the National Oceanic and Atmospheric Administration (NOAA) suggests that the global volume of flared gas exceeds 140 billion m^3 annually, approximately 90% of which is associated with upstream OG production.[6] The sheer magnitude of global gas flaring causes concern for the climate effects of its associated pollutants, especially BC and CO_2. Effects of BC are amplified at higher latitudes, where deposition of BC reduces surface albedo and enhances the melting of snow and ice.[4] Stohl et al.[7] have suggested that 66% of source BC concentrations north of the Arctic circle are from gas flaring, and model data suggest that observed BC concentrations are due in large part to the transport of flare-generated BC from western Siberia.[7,8] Many have thus suggested that gas flaring, especially in the upstream OG industry, is a critical source of BC emissions, despite its relatively small contribution to global emissions.[7,9,10] Moreover, the atmospheric lifetime of BC is very short relative to CO_2, such that the mitigation of BC emissions could enable climatic benefits on a much shorter time scale than current CO_2-reduction efforts,[5,9,11,12] particularly in the developing world.[11]

Unfortunately, BC emissions from gas flaring in the OG industry are poorly characterized and highly uncertain.[7,9,12,13] BC emissions from in-field gas flares have been historically difficult to measure; as such, published emission factors relating BC emission to a quantity of flared gas are necessarily derived from a very limited number of small-scale laboratory and controlled field experiments.[13] Two oft-cited emission factors in the literature are those of the Canadian Association of Petroleum Producers (CAPP[14]) and McEwen and Johnson.[13]

Received: July 22, 2016
Revised: October 31, 2016
Accepted: December 20, 2016
Published: December 20, 2016

DOI: 10.1021/acs.est.6b03690
Environ. Sci. Technol. XXXX, XXX, XXX−XXX

CAPP proposed a $PM_{2.5}$ emission factor of 2.5632 g/m^3 (significant figures as reported) based on a U.S. Environmental Protection Agency (EPA) factor for landfill gas flares attributed to filterable PM measurements conveyed in a confidential report.[15] CAPP adjusted the EPA factor to apply to a higher energy content gas stream, where a value of 45 MJ/m^3 was used to represent the higher heating value (HHV) of associated gas typical of the upstream OG industry. Although not specified, CAPP presumably assumed a linear relationship with HHV to scale up the EPA landfill gas emission factor of ~0.85 g/m^3 (53×10^{-6} lb/ft^3)[15] starting from an approximate HHV of 15 MJ/m^3 for landfill gas.[13] This scaling procedure implies the following BC emission factor (EF) relation: EF[g/m^3] = 0.05696 HHV[MJ/m^3] at standard conditions of 1 atm and 15 °C as used by CAPP[14] and the Intergovernmental Panel on Climate Change (IPCC),[16] with the inherent assumption that within the accuracy of this factor, flare-generated PM is predominantly BC. This is consistent with recent field data[17] suggesting that the presence of non-BC aerosols in a flare plume is "not statistically different from zero", based on absorption measurements downstream of the flame. McEwen and Johnson[13] performed BC yield measurements from lab-scale flares in quiescent laboratory conditions with alkane-based compositions representative of associated gas in Alberta's upstream OG industry. Based on the expected reduction in sooting propensity under crosswind conditions, they proposed a "worst-case" emission factor as a function of HHV via a linear fit to their data: EF[g/m^3] = 0.0548 HHV[MJ/m^3] − 1.98, which has been adjusted for the above-noted standard conditions. Finally, the BC emission factor used by Stohl et al.[7] in the GAINS (greenhouse gas − air pollution interactions and synergies) model[18] is 1.6 g/m^3, derived with data from CAPP,[14] the U.S. EPA,[19] and Johnson et al.[20]

Recently aircraft sampling techniques have been used to estimate BC emissions from flares in the Bakken formation of North Dakota.[17,21] Weyant et al.[17] derived BC emissions factors starting from recorded concentrations of BC, CO_2, and CH_4 during 1−2 s transects of atmospheric flare plumes. An estimated flare gas composition (C1-C15, CO_2, N_2, and other trace species) based on measurements of C1 to C4, H_2S, plus combined diluent species from seven sites in the Bakken region[22] was subsequently used to derive hydrocarbon-mass-based BC emission factors for the flares. The average emission factors of the 26 measured flares spanned 2 orders of magnitude from 0.0023 to 0.33 g/kg hydrocarbons, and the average emission factor for all flares was 0.14 g/kg hydrocarbons. The authors suggested an upper bound for the average emission factor of their measured flares of 0.31 g/kg hydrocarbons based on nonselective absorption measurements of sampled aerosols (although a contradictory value of 3.1 g/kg hydrocarbons appears in their abstract, which is presumably a typographical error). Unfortunately, the measured flares were all nonvisibly smoking and represent a subset of flares with presumably small relative contributions to global BC emissions from flaring. It was also noted that "two flares that were resampled on different days did not maintain consistent BC emission factors", with a provided example varying by a factor of 12.[17] This could point to large variability in the operating conditions of the measured flares and/or could suggest that longer sampling durations (either acquired continuously or as an ensemble of many measurements) are needed to account for the inherently turbulent soot formation and emission process.

This paper presents direct field measurements of BC emission rates from a variety of flares in Ecuador's Orellana province and the state of Veracruz, Mexico. BC emission rates were measured within precisely calculated uncertainties using the recently developed sky-LOSA measurement technique[20,23,24] (line-of-sight attenuation using skylight). The flares in Ecuador were measured during two separate field campaigns, first in June 2014, and subsequently in October 2015. During the latter campaign, parallel measurements of flare gas flow rates in the lines feeding the flares were performed, and extractive samples were drawn for detailed compositional analysis. These data allowed the first direct measurements of fuel-mass-specific BC yields from in-field associated gas flares. Results are compared with the limited available data and emission factor models in the literature, enabling fresh insights into the potential significance of global BC emissions from flaring, the strong influence of flare gas chemistry on relative emission rates, and the importance of absolute emission rate data for identifying reduction opportunities and quantifying mitigation efforts.

METHOD

Measured Flares. Fourteen independent measurements were performed on nine flares located at sites under the jurisdiction of Petróleos Mexicanos in Veracruz, Mexico and Petroamazonas in Orellana, Ecuador. The measured flares in Veracruz included three pit flares, a steam-assisted stack flare, and a steam-assisted enclosed ground flare and were associated with refinery and petrochemical operations. All four measured flares in Orellana were vertical stack flares and were associated with upstream oil production activities. Table 1 summarizes the types of the measured flares, operating conditions, engineered emissions reduction techniques employed, and the naming convention used in this manuscript. Additional details and photographs of the flares are provided in the Supporting Information (SI) to this manuscript. The flares in Orellana were all simple pipe flares fed by one or more lines connected into the base of each flare stack. As noted in the SI, Flare O1 employed a partial-premixing technique at its base in which the input flare line terminated in a vertical-axis nozzle situated below a vertically offset flare stack. It was presumed that this

Table 1. Summary of Flares Measured at OG Sites in Veracruz, Mexico and Orellana, Ecuador

flare	type[a]	nominal stack diameter[b]	simultaneous flow and composition?	operating conditions
V1	pit	n/a	N	~24-h event
V2	ground (SA, E)	n/a	N	steady
V3	pit	n/a	N	steady
V4	stack (SA)	36″	N	unsteady/ control issue
V5	pit	n/a	N	steady
O1	stack (PP)	6″	Y (2015)	steady
O2	stack	12″	Y (2015)	steady[c]
O3	stack	6″	Y (2015)	steady
O4	stack	12″	Y (2015)	steady[c]

[a]SA = steam-assisted; E = enclosed; PP = partially premixed via an air entrainment nozzle arrangement at the base of the flare stack. [b]Measured using sky-LOSA images. [c]One of two lines feeding the flare had variable/oscillating flow but the flame appeared qualitatively steady.

DOI: 10.1021/acs.est.6b03690
Environ. Sci. Technol. XXXX, XXX, XXX−XXX

design was intended to reduce flare-generated BC by entraining ambient air at the base of the stack to mix with the flare gas prior to combustion.

As more fully detailed in the SI, apparent operating conditions and measured flare flow rates where available were reasonably steady for all flares during measurements with the notable exceptions of Flare V1 and Flare V4. Flare V1 experienced a very significant, large-volume, ~24-h flaring event (see the SI) during the field campaign, and three independent BC emission rate measurements were successfully performed on this flare as the event was ending and particulate emissions were in decline. Flare V4 was experiencing an apparent steam control issue that caused slow oscillations in the size of the flame.

Black Carbon Emission Rate – Sky-LOSA Theory. BC emission rates were calculated using sky-LOSA, an imaging technique developed by Johnson et al.[20,23,24] that enables the quantification of the instantaneous BC emission rate from the atmospheric plume of an in situ gas flare. This is accomplished through the analysis of high framerate grayscale image data (over a narrow spectral bandwidth) along an artificial control surface transecting the plume in the image plane. Rayleigh-Debye-Gans theory for Polydisperse Fractal Agglomerates (RDG-PFA, rigorously described by Sorensen[25]) is used to compute line-of-sight (LOS) integrated BC volume fractions along the control surface, which are coupled with velocity measurements using Image Correlation Velocimetry (ICV) to compute the time-resolved BC emission rate. Referring to Johnson et al.[24] for a complete development of sky-LOSA theory, the mass emission rate can be derived via the combination of RDG-PFA and Beer–Lambert law, giving

$$\dot{m} = \frac{\rho\lambda}{6\pi(1+\rho_{sa})E_{(m_\lambda)}}\int \bar{u}[(-\ln\tau^*)]dy = \overline{MEC}^{-1}\int \bar{u}[(-\ln\tau^*)]dy \quad (1)$$

where ρ is the density of BC (i.e., the primary particle density as opposed to the bulk density) [kg·m^{-3}], λ is the measurement wavelength [m], ρ_{sa} is the ratio of aggregate-average scattering and absorption cross-sections [−], $E_{(m_\lambda)}$ is the spectrally dependent absorption index of refraction function for flame-generated BC [−], $\bar{u}$is the volume fraction-weighted particle velocity normal to the control surface along the LOS [m·s^{-1}], and τ^* is the LOS-transmittance that would be observed absent of in-scattering effects from ambient radiation (i.e., the idealized transmissivity presented by Johnson et al.[24]) [−]. As shown in eq 1, the reciprocal of terms outside the integral represents the mass extinction cross-section of the average particle ($\overline{MEC}$) along the LOS axis [m^2·g^{-1}] calculated considering polydispersity.

For a sky-LOSA measurement subject to in-scattering of hemispherical skylight and solar radiation, the idealized transmissivity can be derived through consideration of a control volume spanning the LOS axis.[24] Solution of the resulting differential equation yields

$$\tau^* = \left(\tau_{\exp} - \frac{B+C}{AI^0_{LOS}}\right)\left(1 - \frac{B+C}{AI^0_{LOS}}\right)^{-1} \quad (2)$$

where $\tau_{\exp}$ is the field-measured transmittance of the plume (including in-scatter components) [−], I^0_{LOS} is the unobstructed LOS skylight intensity [W·m^{-2}·sr^{-1}], $A = \overline{\sigma_{ext}}$ is the extinction cross-section of the average aggregate [m^2], $B = \int_{2\pi} I_{sky}\overline{\sigma'_{sca_{(\theta)}}}d\Omega$ quantifies the in-scattered radiant intensity of hemispheric skylight by the average aggregate [W·sr^{-1}], $C = E_{sun}\overline{\sigma'_{sca(\theta_{sun})}}$ quantifies the in-scattered radiant intensity of solar radiation by the average aggregate [W·sr^{-1}], $\overline{\sigma'_{sca_{(\theta)}}}$ is the angular differential scattering cross-section of the average particle (including *vv*- and *hh*-polarization components) [m^2·sr^{-1}], and θ is the scattering angle of incident radiation relative to the LOS [rad].

BC from turbulent diffusion flames, such as gas flares, are known to exist as mass-fractal-like aggregates of constant size nanoscale spherules.[26−28] Consequently, parameters based on the average particle (calculated using RDG-PFA) are evaluated over a polydisperse fractal aggregate size distribution.

Black Carbon Emission Rate – Sky-LOSA Implementation. The present sky-LOSA field measurements of BC emission rate were implemented as in Johnson et al.,[24] apart from the following hardware upgrades and algorithmic enhancements implemented for the measurements in Ecuador. High framerate grayscale image data for sky-LOSA analysis were acquired in-field using the scientific-CMOS sky-LOSA camera (pco, Edge 5.5). During previous measurements[24] and the present measurements in Mexico, image data were written directly to the field-computer's RAM at approximately 0.5 GB/s, which limited full-sensor acquisition times to less than one minute. For the present measurements in Ecuador however, field-hardware was upgraded to include 1 TB of flash storage enabling multiple ten minute acquisitions before offloading was necessary. This upgrade enabled the calculation of mean BC emission rates over significantly longer sampling times to better capture the nonstationary behavior of emissions and provide robust time-averaged emissions data. Upgraded software (LaVision, DaVis v.8.2.3) used to obtain the volume fraction-weighted mean velocity along the LOS-axis allowed more rigorous estimation of velocity field uncertainty based on correlation statistics between the first image in the ICV pair and the second image dewarped using the computed velocity field.[29] This additional functionality provides a more robust estimation of uncertainty in the BC emission rate associated with the determination of plume velocity. Both a standard and a Combined Multiple Latin Hypercube Sampled Monte Carlo (MC) method as described by Nakayama[30] (used where applicable to reduce computation time) were used to rigorously calculate experimental uncertainties. As further detailed in the SI, MC calculations used probability distributions[24] of physical, morphological, and optical properties of flame-generated BC aggregates as well as uncertainties in plume velocity and background sky reconstruction to compute uncertainties in BC emission rate, such that the coefficient of variation for all computed percentiles within the 95% equal tail confidence interval was less than 0.34%.

Flare Gas Flow Rate Measurement. Simultaneous measurements of flare gas flow rate were performed during the 2015 measurements in Ecuador's Orellana province to enable calculation of BC yields for the measured flares. Standard conditions of 1 atm and 15 °C are adopted in the present study in accordance with the IPCC[31] and CAPP;[14] hereinafter, units of cubic meters [m^3] are defined to be at these conditions. Existing emission factors in the literature have been adjusted to these standard conditions for comparison with current data.

DOI: 10.1021/acs.est.6b03690
Environ. Sci. Technol. XXXX, XXX, XXX−XXX

Two complementary flare gas flow rate measurement techniques were used: a tracer-dilution technique and an optical velocity measurement technique. The tracer-dilution technique employed a mass flow controller (Brooks, SLAMF50S) to inject negligibly small volumes of a stable tracer (acetylene) into the turbulent flare lines at a known rate. At a position sufficiently downstream of the injection point, a cavity ring-down instrument (Los Gatos Research, 915-0043) was used to continuously sample and measure tracer gas concentration in the fully mixed flare gas-tracer gas mixture. Molar continuity (assuming tracer stability) was used to compute flare gas standard volumetric flow rate with knowledge of flare and tracer gas properties. Injection and sampling were performed via 1/4″-diameter stainless steel insertion probes; each 1/4″ probe had two orthogonal rows of 15 1/32″-diameter holes drilled along its length that spanned the flare line diameter. The probes were positioned so that the rows of holes were aligned at 45° to the bulk flow direction to promote rapid mixing of the injected tracer or to ensure representative sampling.

For the optical velocity measurement technique, an optical flow meter (OFM, Photon Control, Focus 2.0) was used to measure the flare gas velocity at the center of the flare line. With knowledge of flare gas properties, dimensions of the flare line, and an assumed axisymmetric velocity profile, the flow rate of flare gas was calculated. In some instances, OFM measurements of raw velocity were corroborated using an insertion vane wheel anemometer (Höntzsch, ZS18GE-mc40). To support flow rate calculations using the optical velocity measurement technique, flare gas pressure and temperature data were acquired via an absolute digital pressure gauge (Additel, ADT 681) and a 4-wire Pt100 platinum resistance thermometer (Höntzsch, TF500).

Flare Gas Composition. To enable direct calculation of BC yields and to provide insight into their sensitivity to fuel composition and chemistry, extractive gas samples were acquired from relevant flare lines for off-site analysis. Highly resolved gas chromatographic analyses (test method: CAN/CGSB-3.0 No. 14.3-99[32]) were contracted to obtain volume fractions of alkanes to C_{15}; alkenes to C_{10}; cycloalkanes and aromatics to C_{12}; other combustibles (H_2 and H_2S); and diluents (He, CO_2, and N_2). Full composition details are included in the SI.

RESULTS

Black Carbon Emissions. Figure 1 shows the time-averaged BC emission rates of all in-field flares measured using sky-LOSA to date. Included are measurements in Uzbekistan;[20] Poza Rica, Mexico;[24] and the 14 measurements of the nine flares constituting the current data set. Field-measured time-averaged BC emission rates in the current data set ranged from 0.003 g/s to 53.7 g/s and include the lightest and heaviest sooting flares that have been measured using sky-LOSA.

As discussed in the SI, the time-resolved BC emission rate data for each flare were highly stochastic. All but one flare were statistically trend nonstationary (at a 5% significance level using the Kwiatkowski-Phillips-Schmidt-Shin test[33]) and exhibited positive skewness (with a mean and maximum sample skewness of 1.04 and 3.21). An example of this stochastic nature is shown in Figure 2, where a 5 s subset of instantaneous BC emission rate data from Flare O3 measured in 2015 is plotted along with 95% confidence intervals computed using the described MC

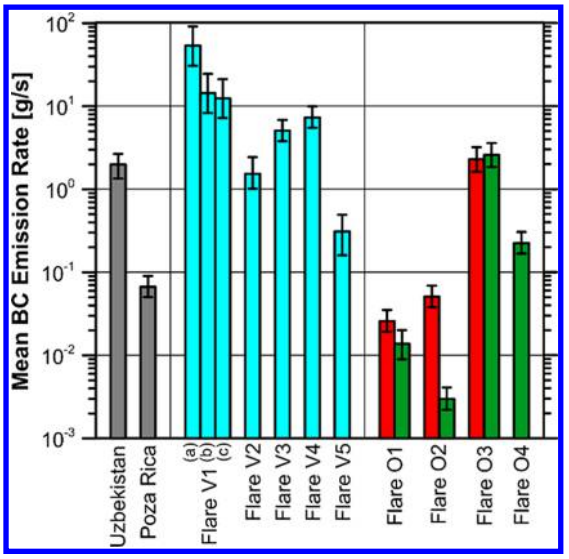

Figure 1. Absolute mean BC emission rates measured using sky-LOSA in g/s. Gray bars represent previous measurements in Uzbekistan[20] and Poza Rica, Mexico,[24] while the 14 colored bars represent measurements in Veracruz, Mexico in 2012 (cyan) and Orellana, Ecuador in 2014 (red) and 2015 (green). Note the logarithmic scale on the vertical axis which is necessary to capture the large variation of emission rates among flares.

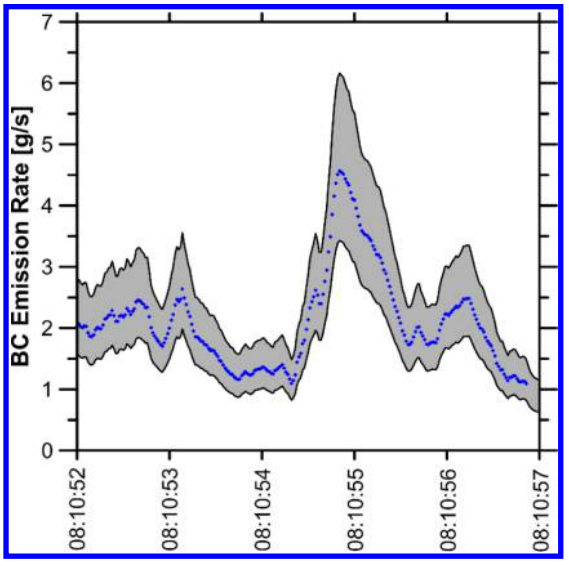

Figure 2. A 5 s subset of measured instantaneous BC emission rate (calculated at 50 Hz) from Flare O3 in 2015 showing high variability. The blue symbols represent the instantaneous mean, and the shaded region represents the 95% confidence interval computed using the MC methodology.

methodology. As further discussed in the SI, in the most extreme case (Flare O2 as measured in 2015), the inherent variability of the BC emission rate was to the extent that 10% of the instantaneous data were responsible for 56% of total emissions. These observations imply that BC emissions from flares are heavily weighted by intermittent bursts of optically dense structures within the plume, which suggests that long-duration measurements are necessary to obtain robust average emission metrics and future measurements should strive to maximize measurement duration. Coupled with the more than 4 orders of magnitude variation in mean BC emission rates

DOI: 10.1021/acs.est.6b03690
Environ. Sci. Technol. XXXX, XXX, XXX−XXX

Table 2. Summary of Flare Gas Compositions of the Measured Flares by Chemical Group with Key Flare Gas Properties Relevant to BC Emissions from Turbulent Diffusion Flames[b]

composition	flare O1[a]	flare O2	flare O3	flare O4	Alberta[34]	Bakken[22]
diluents − CO_2	12.64	9.19	5.69	6.30	1.41	0.57
diluents − N_2	8.17	5.74	3.35	4.11	3.35	5.21
alkanes	78.10	84.46	89.80	88.79	94.85	94.19
cycloalkanes	0.57	0.46	1.05	0.68		
alkenes and cycloalkenes	0.46	0.08	0.04	0.06		
aromatics	0.02	0.02	0.05	0.02		
other combustibles	0.01	0.03	0	0.04		
property						
molecular weight, [kg/kmol]	31.57	27.73	36.61	30.33	19.21	25.19
carbon-to-hydrogen ratio	0.361	0.336	0.366	0.344	0.273	0.310
fraction of hydrocarbons that were unsaturated, $\%_{v/v}$	0.61	0.12	0.10	0.10		
higher heating value, [MJ/m^3]	51.80	48.87	71.29	57.77	38.236	55.11

[a]Measured in the line feeding Flare O1. As noted earlier, Flare O1 employed an air entrainment system at the base of the flare stack such that an unquantified amount of air would have been mixed into the flare gas prior to combustion at the flare exit. [b]Also shown are mean associated gas compositions from oil and bitumen batteries in Alberta's upstream OG industry[34] and an assumed mean associated gas composition from the Bakken region.[22]

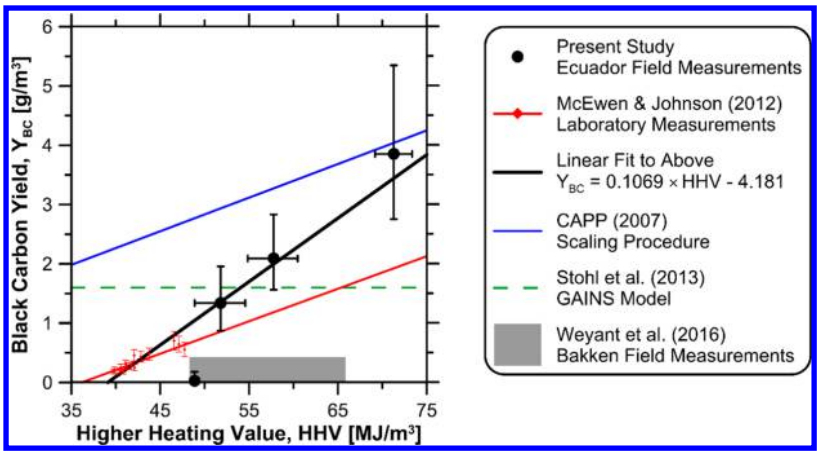

Figure 3. Mean and 95% confidence interval of measured BC yields on a mass-per-volume basis shown as a function of volumetric higher heating value. Included are the predictive emission factors using the heating value scaling procedure of CAPP,[14] the correlation developed by McEwen and Johnson,[13] and the emission factor currently used in the GAINS model;[7] also shown is the estimated range of yield measurements in the Bakken region by Weyant et al.[17] based on the span of reported measurements[17] converted from mass-per-mass of hydrocarbons to mass-per-volume of flare gas using the cited range of gas compositions.[22]

among the measured flares, this highlights how aggregate emissions can be dominated by outliers and underscores the importance of quantitative measurements in identifying mitigation opportunities. Indeed, action to reduce or eliminate a flare like V1 (emitting BC continuously at the maximum measured rate) would have equivalent BC reductions to mitigating almost 18,000 flares similar to O2 (as measured in 2015). Alternately stated, Flare V1 operating at the maximum measured rate for one day (which as noted in the SI is likely much lower than the peak emission rate during the 24-h flaring event) produces equivalent BC emissions to more than 49 flares similar to O2 (as measured in 2015) operating continuously for *a year*.

Flare Gas Composition. Table 2 shows the measured associated gas compositions by chemical group and key properties of flared volumes relevant to the propensity of BC emissions from turbulent diffusion flames − refer to the SI for a detailed summary of flare gas composition. For context, Table 2 includes data representative of associated gas compositions at oil and bitumen batteries in Alberta (derived from 60,000+ gas samples[34]) and an assumed mean composition from the Bakken region[22] used in Weyant et al. analysis.[17] As noted in the footnotes of Table 2 and further discussed in the SI, downstream of the sampling point, Flare O1 incorporated an air entrainment nozzle at the base of the flare stack such that the degree of partial premixing of flare gas and air within the flare stack was unknown.

While the associated gases in Ecuador's Amazon basin contained heavier alkane mixtures (resulting in a higher energy content and a greater carbon-to-hydrogen ratio) than associated gases in Alberta and the Bakken region, they were also significantly more diluted with CO_2 and N_2. The current data illustrate that flare gas composition can vary significantly within small geographic areas, which was also observed in Alberta and the Bakken region, where total diluent fractions as high as 29.1% and 19.8% were observed, respectively, despite averages of less than 6%. As the literature has shown that BC emissions from diffusion flames are most sensitive to dilution,[35,36] aeration,[37] energy content of the fuel,[13] and the relative fraction of unsaturated hydrocarbons (often quantified using the fuel's carbon-to-hydrogen ratio),[19] it is imperative that future field-measured BC emission factors are interpreted in the

DOI: 10.1021/acs.est.6b03690
Environ. Sci. Technol. XXXX, XXX, XXX−XXX

context of matching flare gas composition data. Moreover, highly detailed compositional analyses are required to resolve unsaturated components, which can strongly influence sooting propensity; unfortunately, although these compounds have been observed in small amounts in crude oil across the globe, petroleum geochemists do not commonly analyze for such compounds.[38]

Black Carbon Yields. Field-measured BC yields in Ecuador are shown in Figure 3 as a function of volumetric HHV with 95% confidence intervals computed using the MC methodology detailed in the SI. A potential range of BC yields from the measurements of Weyant et al.[17] in the Bakken region is shown as a shaded area on the graph, where data have been converted from a mass of hydrocarbons basis to a volume of flare gas basis using the cited range of flare gas compositions of seven flares in the Bakken[22] and are plotted spanning the range of heating values in these same samples. The measured BC yields in Ecuador spanned more than 2 orders of magnitude from 0.03 to 3.85 g/m^3 (refer to the SI for site-specific results) with an average of 1.83 g/m^3. The heaviest-sooting flare was ∼27 times greater than the estimated average for the Bakken region,[17] while only the lightest-sooting flare was within the range of those same measurements.

Overlaid in Figure 3 are a prediction of BC yield as a function of HHV using the simple scaling procedure implemented by CAPP,[14] the experimental data and empirical correlation derived by McEwen and Johnson,[13] and the current GAINS model emission factor.[7] The CAPP scaling procedure tends to overestimate the measured yields, although the heaviest sooting flare (O3) approached the CAPP prediction. Given that the CAPP factor is ultimately extrapolated from a single measurement on a (potentially enclosed) landfill gas flare at ∼15 MJ/m^3, it is not surprising that the prediction fails at much higher heating values. Alternatively, McEwen and Johnson's correlation, derived using the data points reproduced in red on the figure, underestimated the BC yield for three of the measured flares at greater HHV. Although HHV has been observed in laboratory experiments[39] to dominate other effects by order(s) of magnitude, the sooting propensity of turbulent diffusion flames is known to be sensitive to ambient conditions, aerodynamic parameters, and other chemistry metrics, many of which happen to have a positive correlation with HHV. Consequently, this presentation of the results is not intended to suggest that BC emission factor is solely a function of flare gas energy content but instead highlights the utility of this parametrization as a starting point. Within this context, recognizing the pragmatic need for measurement-backed models, the black line shows an empirical fit to available laboratory[13] and field data for black carbon yields from flares as a function of HHV. The coefficient of determination (R^2) for this line is 0.896. Interestingly, if published associated gas compositions from nearby Alberta[34] were representative of flares measured by Weyant et al.,[17] their data would align quite well with this model as well as the data of McEwen and Johnson,[13] perhaps suggesting that the assumed composition of Weyant et al.[17] overestimates the actual heating value of their measured flares. Moreover, as further discussed in the SI, Flare O2 (corresponding to the lowest data point included in this correlation) might be reasonably considered an outlier relative to other flares, due to its highly nonstationary nature linked with variable flow in one of its supply lines that resulted in large gaps of nondetectable emissions. Without this point included, both the slope and R^2-value of the fit would increase (Y_{BC} = 0.1106 × HHV − 4.296, R^2 = 0.966).

Implications. To date, 16 absolute BC emission rate measurements have been performed on 11 flares using sky-LOSA, with the results spanning more than 4 orders of magnitude. At least one flare has also been observed however, with plume BC concentrations sufficiently high such that direct solar radiation could not penetrate the plume. This suggests that BC emissions from flaring span an even larger range due to the presence of superemitters. The existence of such drastic flaring events supports the notion that superemitters must be targeted when performing measurements to support the improved estimation of emissions inventories and enable effective mitigation efforts. It also begs the question of the global distribution of absolute emission rate, where the relative contribution to global BC emissions from non- or lightly visibly sooting flares might be considered negligible. It is therefore important to consider absolute emission rates in addition to flare-gas-specific yields (measured in conjunction with parallel flare gas flow rate and composition data) when directing mitigation actions to optimize emissions reduction efforts. Consistent with the literature noting the nonlinear intensity perception[40] and nonuniform spectral sensitivity[41] of the human eye, field experience has shown that qualitative visual assessment of emissions is a poor surrogate for quantified emission rates.

The current data set also demonstrates that flare gas compositions can be quite diverse even in small geographic regions, and this diversity can have a significant impact on BC yield. This unfortunately complicates efforts to predict regional or global emissions without considering compositional variations in flare gas.

As of 2013, the GAINS model estimates global BC emissions from gas flaring by coupling calculated flared volumes using satellite imagery from NOAA (including work by Elvidge et al.[42]) and a BC emission factor of 1.6 g/m^3,[7] which is a factor of 3 greater than McEwen and Johnson's[13] proposed emission factor for typical associated gas compositions in Alberta. Stohl et al.[7] contend however that "even when using the emission factor from McEwen and Johnson, gas flaring remains the second largest source of BC emissions north of 60°N and the most important anthropogenic source". Stohl et al.[7] then suggest that the correlation of McEwen and Johnson likely underestimates equivalent emissions from in-field flares, presumably due to the difficulty in recreating complex compositions containing the heavier alkanes and unsaturated hydrocarbons observed in the OG industry within the laboratory. In contrast, Weyant et al.[17] note that if the average BC yield from their measurements in the Bakken region is spatially and temporally representative of global flaring (the authors do however emphasize that their measurements were limited to nonvisibly sooting flares), then the GAINS model emission factor is more than an order of magnitude high. However, if a similar approach is taken, then the present field measured BC yields would suggest that the emission factor used within the GAINS model is ∼10% low. This highlights the limited utility of a simple mean BC yield derived from small data sets in small geographic regions.

Recently, Huang et al.[43] performed independent simulations of anthropogenic BC transport from Russia to the Arctic. In place of the GAINS value, an emission factor for gas flaring was estimated by extrapolating the relation of McEwen and Johnson[13] to a representative HHV derived from an example

DOI: 10.1021/acs.est.6b03690
Environ. Sci. Technol. XXXX, XXX, XXX−XXX

associated gas composition from a Russian oil field by Filippov.[44] Flare gas composition was computed as a weighted sum of flared gases from three stages of oil separation. Although additional data were available for oil and gas producing sites (with significantly lower heating values), Huang et al.[43] argued that the oil field composition was a better representation for the OG industry in Russia as it has been noted elsewhere[45] that most associated gas in Russia has a methane content less than 50%. A median HHV of 75.5 MJ/m^3 was calculated, yielding an emission factor of 2.27 g/m^3, and applied to an estimated 35.6 billion m^3 flared in Russia per year (using NOAA data from 2010). Huang et al.[43] concluded that gas flaring is responsible for 36.2% of Russia's anthropogenic BC emissions, the largest contributor by more than 10%. However, it has been observed in the present study that McEwen and Johnson's emission factor relation is low at greater HHVs, and if the assumed gas composition for Russia (with a recomputed mean HHV of 71.5 MJ/m^3 ± 2.5% at standard conditions as defined) were in line with the trend observed in the current study, it is possible that a more appropriate emission factor using the derived linear fit to the current field measurements and lab data of McEwen and Johnson[13] would be approximately 3.46 g/m^3. Thus reconsidering the work of Huang et al.[43] in the context of the present field measurements on larger heating value flares would suggest that flaring-related BC emissions from Russia could be on the order of 123 Gg/year or as much as ∼46% of Russia's anthropogenic BC emissions.

Although the authors are not aware of a reliable source for a globally representative heating value for flared gas, as an initial starting point for discussion (see the SI for calculation details), if one were to use satellite derived flaring data for Canada, USA, Russia, and Ecuador[6] to weight available flare gas composition data[22,34,43] for each country, and assuming an arithmetic mean of these data for other countries in the world, a representative global flare gas heating value could be ∼60.03 MJ/m^3. Based on the proposed BC yield model in Figure 3, this would imply a global mean BC emission factor of 2.24 g/m^3 (40% higher than the emission factor used in the GAINS model). Alternatively, if the volume-weighted average value of 67.23 MJ/m^3 for the four countries with available data were considered globally relevant, then the proposed BC model would imply a global mean BC emission factor of 3.01 g/m^3, suggesting the GAINS model emission factor could be low by almost a factor of 2. While these estimates are subject to significant uncertainty, they stress the importance of accurate BC emission factor data in characterizing the scale of global BC emissions from flaring. Ultimately, accurate prediction of global flare BC emissions will require significantly augmented field measurement data (specifically including simultaneous measurements of flare gas composition and flow rates) coupled with comprehensive models building on the simple correlation presented here.

Most importantly, the presented direct field measurement data have provided evidence of the extreme variability in emission rates among flares (see Figure 1), the potential for individual flares to be very significant single sources of BC, and the strong correlation of volume-specific BC yields with flare gas heating value. Further field measurements are certainly desired to improve upon the presented emission factor relation by introducing additional flare design, operation, and chemistry metrics, where the demonstrated implications justify the need to overcome continued challenges of gaining necessary site access to quantify flare gas flow rate and composition in conjunction with parallel BC emission rate measurements. Nevertheless, if the current results are interpreted in the context of recent efforts to track impacts of flare-generated BC in the Arctic and globally,[7,43] it could be the case that the significant global public health and climatic impacts of BC emissions from gas flaring in the OG industry are in fact underestimated.

■ ASSOCIATED CONTENT

Supporting Information

The Supporting Information is available free of charge on the ACS Publications website at DOI: 10.1021/acs.est.6b03690.

Details of the measured flares; summaries of all acquired data and further details on the measurement methodology and Monte Carlo based uncertainty analysis; tabulated data for BC emission rates, flare compositions, flow rates, and derived BC yield data, all with associated uncertainties; plotted distributions and additional statistics of the time-resolved BC rate data; and background information used to estimate a representative global flare gas heating value (PDF)

■ AUTHOR INFORMATION

Corresponding Author

*Phone: 613-520-2600 ext. 4039. E-mail: Matthew.Johnson@carleton.ca.

ORCID

Bradley M. Conrad: 0000-0003-3678-7434

Notes

The authors declare no competing financial interest.

■ ACKNOWLEDGMENTS

This work was supported by the World Bank Global Gas Flaring Reduction Partnership (Project Manager Francisco Sucre), the United Nations Environment Programme's Climate and Clean Air Coalition (Project Manager Joseph Odhiambo), Natural Resources Canada (Project Manager Michael Layer), the Petroleum Technology Alliance of Canada (Grant #09-9185-50), and the Natural Sciences and Engineering Research Council of Canada (NSERC, Grant #261966, 446199, and 479641). We are especially thankful for the assistance received during field measurements in Ecuador from Petroamazonas personnel including David Neira, Javier Villacis, and David Herrera, as well as from Melina Jefferson and Darcy Corbin (Carleton University). Measurements in Mexico were possible through on the ground support and assistance of Robin Devillers (National Research Council of Canada), Michael Layer, David Picard (Clearstone Engineering Ltd.), Javier Bocanegra (Pemex), and Jorge Plauchú (independent consulting engineer). Finally, we are indebted to Berend van den Berg (Power Latinamerica Inc.) and Kevin Thomson (National Research Council of Canada) for their support in making these field measurements possible.

■ REFERENCES

(1) Grahame, T. J.; Klemm, R.; Schlesinger, R. B. Public health and components of particulate matter: The changing assessment of black carbon. *J. Air Waste Manage. Assoc.* **2014**, *64* (6), 620−660.

(2) Kim, S.-Y.; Dutton, S. J.; Sheppard, L.; Hannigan, M. P.; Miller, S. L.; Milford, J. B.; Peel, J. L.; Vedal, S. The short-term association of selected components of fine particulate matter and mortality in the Denver Aerosol Sources and Health (DASH) study. *Environ. Health* **2015**, *14* (1), 49.

DOI: 10.1021/acs.est.6b03690
Environ. Sci. Technol. XXXX, XXX, XXX−XXX

(3) Basagaña, X.; Jacquemin, B.; Karanasiou, A.; Ostro, B.; Querol, X.; Agis, D.; Alessandrini, E.; Alguacil, J.; Artiñano, B.; Catrambone, M.; et al. Short-term effects of particulate matter constituents on daily hospitalizations and mortality in five South-European cities: Results from the MED-PARTICLES project. *Environ. Int.* **2015**, *75*, 151−158.
(4) Jacobson, M. Z. Short-term effects of controlling fossil-fuel soot, biofuel soot and gases, and methane on climate, Arctic ice, and air pollution health. *J. Geophys. Res.* **2010**, *115* (D14209), 1−24.
(5) Bond, T. C.; Doherty, S. J.; Fahey, D. W.; Forster, P. M.; Berntsen, T.; DeAngelo, B. J.; Flanner, M. G.; Ghan, S.; Kärcher, B.; Koch, D.; et al. Bounding the role of black carbon in the climate system: A scientific assessment. *J. Geophys. Res. Atmos.* **2013**, *118* (11), 5380−5552.
(6) Elvidge, C. D.; Zhizhin, M.; Baugh, K.; Hsu, F.; Ghosh, T. Methods for Global Survey of Natural Gas Flaring from Visible Infrared Imaging Radiometer Suite Data. *Energies* **2016**, *9* (1), 14.
(7) Stohl, A.; Klimont, Z.; Eckhardt, S.; Kupiainen, K.; Shevchenko, V. P.; Kopeikin, V. M.; Novigatsky, A. N. Black carbon in the Arctic: the underestimated role of gas flaring and residential combustion emissions. *Atmos. Chem. Phys.* **2013**, *13* (17), 8833−8855.
(8) Stohl, A. Characteristics of atmospheric transport into the Arctic troposphere. *J. Geophys. Res.* **2006**, *111* (D11306), 1−17.
(9) U.S. EPA. *Report to Congress on Black Carbon*; EPA-450/R-12-001; United States Environmental Protection Agency (U.S. EPA): Research Triangle Park, NC, 2012.
(10) Ramanathan, V.; Carmichael, G. Global and regional climate changes due to black carbon. *Nat. Geosci.* **2008**, *1* (4), 221−227.
(11) Kopp, R. E.; Mauzerall, D. L. Assessing the climatic benefits of black carbon mitigation. *Proc. Natl. Acad. Sci. U. S. A.* **2010**, *107* (26), 11703−11708.
(12) IPIECA. *Understanding short-lived climate forcers*; London, UK, 2014.
(13) McEwen, J. D. N.; Johnson, M. R. Black Carbon Particulate Matter Emission Factors for Buoyancy Driven Associated Gas Flares. *J. Air Waste Manage. Assoc.* **2012**, *62* (3), 307−321.
(14) CAPP. *A Recommended Approach to Completing the National Pollutant Release Inventory (NPRI) for the Upstream Oil and Gas Industry*; 2007−0009; 2007.
(15) U.S. EPA. *Data from landfill gas flare, Confidential Report No. ERC-55*; United States Environmental Protection Agency (U.S. EPA): 1991.
(16) IPCC. *Guidelines for National Greenhouse Gas Inventories*; 2006.
(17) Weyant, C. L.; Shepson, P. B.; Subramanian, R.; Cambaliza, M. O. L.; Heimburger, A.; Mccabe, D.; Baum, E.; Stirm, B. H.; Bond, T. C. Black carbon emissions from associated natural gas flaring. *Environ. Sci. Technol.* **2016**, *50* (4), 2075−2081.
(18) Amann, M.; Bertok, I.; Borken-Kleefeld, J.; Cofala, J.; Heyes, C.; Höglund-Isaksson, L.; Klimont, Z.; Nguyen, B.; Posch, M.; Rafaj, P.; et al. Cost-effective control of air quality and greenhouse gases in Europe: Modeling and policy applications. *Environ. Model. Softw.* **2011**, *26* (12), 1489−1501.
(19) U.S. EPA. *AP 42 - Compilation of Air Pollutant Emission Factors, Volume I, 5th ed. - Section 13.5 Industrial Flares*; AP-42; United States Environmental Protection Agency (U.S. EPA): Research Triangle Park, NC, 1995.
(20) Johnson, M. R.; Devillers, R. W.; Thomson, K. A. Quantitative Field Measurement of Soot Emission from a Large Gas Flare Using Sky-LOSA. *Environ. Sci. Technol.* **2011**, *45* (1), 345−350.
(21) Schwarz, J. P.; Holloway, J. S.; Katich, J. M.; McKeen, S.; Kort, E. A.; Smith, M. L.; Ryerson, T. B.; Sweeney, C.; Peischl, J. Black Carbon Emissions from the Bakken Oil and Gas Development Region. *Environ. Sci. Technol. Lett.* **2015**, *2* (10), 281−285.
(22) Wocken, C. A.; Stevens, B. G.; Almlie, J. C.; Schlasner, S. M. *End-Use Technology Study − An Assessment of Alternative Uses for Associated Gas*; 2013.
(23) Johnson, M. R.; Devillers, R. W.; Yang, C.; Thomson, K. A. Sky-Scattered Solar Radiation Based Plume Transmissivity Measurement to Quantify Soot Emissions from Flares. *Environ. Sci. Technol.* **2010**, *44* (21), 8196−8202.
(24) Johnson, M. R.; Devillers, R. W.; Thomson, K. A. A Generalized Sky-LOSA Method to Quantify Soot/Black Carbon Emission Rates in Atmospheric Plumes of Gas Flares. *Aerosol Sci. Technol.* **2013**, *47* (9), 1017−1029.
(25) Sorensen, C. M. Light Scattering by Fractal Aggregates: A Review. *Aerosol Sci. Technol.* **2001**, *35* (2), 648−687.
(26) Köylü, Ü. Ö.; Faeth, G. M. Structure of overfire soot in buoyant turbulent diffusion flames at long residence times. *Combust. Flame* **1992**, *89* (2), 140−156.
(27) Köylü, Ü. Ö.; Faeth, G. M.; Farias, T. L.; Carvalho, M. G. Fractal and projected structure properties of soot aggregates. *Combust. Flame* **1995**, *100* (4), 621−633.
(28) Faeth, G. M.; Köylü, Ü. Ö. Soot morphology and optical properties in nonpremixed turbulent flame environments. *Combust. Sci. Technol.* **1995**, *108* (4−6), 207−229.
(29) Wieneke, B. PIV uncertainty quantification from correlation statistics. *Meas. Sci. Technol.* **2015**, *26* (7), 074002.
(30) Nakayama, M. K. Asymptotically Valid Confidence Intervals for Quantiles and Values-at-Risk When Applying Latin Hypercube Sampling. *Int. J. Adv. Syst. Meas* **2011**, *4* (1), 86−94.
(31) IPCC. *Guidelines for National Greenhouse Gas Inventories - Chapter 4: Fugitive Emissions*; Eggleston, S., Buendia, L., Miwa, K., Mgara, T., Tanabe, K., Eds.; Intergovernmental Panel on Climate Change (IPCC): Hayama Japan, 2006.
(32) Standards Council of Canada. *CAN/CGSB-3.0 No. 14.3-99 Methods of testing petroleum and associated products standard test method for the identification of hydrocarbon components in automotive gasoline using gas chromatography*; 1999.
(33) Kwiatkowski, D.; Phillips, P. C. B.; Schmidt, P.; Shin, Y. Testing the null hypothesis of stationarity against the alternative of a unit root. *J. Econom.* **1992**, *54* (1−3), 159−178.
(34) Johnson, M. R.; Coderre, A. R. Compositions and greenhouse gas emission factors of flared and vented gas in the western Canadian sedimentary basin. *J. Air Waste Manage. Assoc.* **2012**, *62* (9), 992−1002.
(35) Gülder, Ö. L.; Snelling, D. R. Influence of nitrogen dilution and flame temperature on soot formation in diffusion flames. *Combust. Flame* **1993**, *92* (1−2), 115−124.
(36) Glassman, I. Sooting laminar diffusion flames: Effect of dilution, additives, pressure, and microgravity. *Symp. Combust., [Proc.]* **1998**, *27* (1), 1589−1596.
(37) Gülder, Ö. L. Effects of oxygen on soot formation in methane, propane, and n-Butane diffusion flames. *Combust. Flame* **1995**, *101* (3), 302−310.
(38) Curiale, J. A.; Frolov, E. B. Occurrence and origin of olefins in crude oils. A critical review. *Org. Geochem.* **1998**, *29* (1−3), 397−408.
(39) Corbin, D. J. Methodology and Experiments to Determine Soot and NOx Yields from a Vertical Lab-Scale Flare Burning Alkane-Mixtures and Ethylene. M.A.Sc. Thesis, Carleton University, 2014.
(40) Stevens, S. S. On the psychophysical law. *Psychol. Rev.* **1957**, *64* (3), 153−181.
(41) CIE. *2-degree spectral luminous efficiency for photopic vision*; Vienna, Austria, 1990.
(42) Elvidge, C. D.; Baugh, K. E.; Tuttle, B. T.; Howard, A. T.; Pack, D. W.; Milesi, C.; Erwin, E. H. *A Twelve Year Record of National and Global Gas Flaring Volumes Estimated Using Satellite Data: Final Report to the World Bank*; 2007.
(43) Huang, K.; Fu, J. S.; Prikhodko, V. Y.; Storey, J. M.; Romanov, A.; Hodson, E. L.; Cresko, J.; Morozova, I.; Ignatieva, Y.; Cabaniss, J. Russian anthropogenic black carbon: Emission reconstruction and Arctic black carbon simulation. *J. Geophys. Res. Atmos.* **2015**, *120* (21), 11,306−11,333.
(44) Filippov, A. Chemical composition of associated gas. *Neftegaz.ru Magazine*. October **2013**, pp 22−26.
(45) PFC Energy. *Using Russia's Associated Gas: Prepared for the Global Gas Flaring Reduction Partnership and the World Bank*; 2007.

DOI: 10.1021/acs.est.6b03690
Environ. Sci. Technol. XXXX, XXX, XXX−XXX